An allometric relationship between mitotic spindle width, spindle length, and ploidy in *Caenorhabditis elegans* embryos

Yuki Hara* and Akatsuki Kimura
Cell Architecture Laboratory, Structural Biology Center, National Institute of Genetics, and Department of Genetics, School of Life Science, Graduate University for Advanced Studies (Sokendai-Mishima), Yata 1111, Mishima, Shizuoka 411-8540, Japan

ABSTRACT **The mitotic spindle is a diamond-shaped molecular apparatus crucial for chromosomal segregation. The regulation of spindle length is well studied, but little is known about spindle width. Previous studies suggested that the spindle can self-organize to maintain a constant aspect ratio between its length and width against physical perturbations. Here we determine the widths of metaphase spindles of various sizes observed during embryogenesis in *Caenorhabditis elegans*, including small spindles obtained by knocking down the *tpxl-1* or *spd-2* gene. The spindle width correlates well with the spindle length, but the aspect ratio between the spindle length and spindle width is not constant, indicating an allometric relationship between these parameters. We characterize how DNA quantity (ploidy) affects spindle shape by using haploid and polyploid embryos. We find that the length of the hypotenuse, which corresponds to the distance from the apex of the metaphase plate to the spindle pole, remains constant in each cell stage, regardless of ploidy. On the basis of the quantitative data, we deduce an allometric equation that describes the spindle width as a function of the length of the hypotenuse and ploidy. On the basis of this equation, we propose a force-balance model to determine the spindle width.**

Monitoring Editor
Alex Mogilner
University of California, Davis

Received: Jul 18, 2012
Revised: Feb 13, 2013
Accepted: Feb 27, 2013

INTRODUCTION

The mechanisms regulating the sizes of supramolecular complexes inside the cell, such as membrane-bound organelles and mitotic spindles, are important in cell biology because the sizes of these complexes are usually many orders of magnitude larger than those of the constituent macromolecules (Hara and Kimura, 2011). Several mechanisms control the size of intracellular structures (Katsura, 1990; Marshall, 2004; Kalab and Heald, 2008; Levy and Heald, 2010; Moseley *et al.*, 2009; Varga *et al.*, 2009). Of interest, the size of some complexes correlates with the size of others; for example, it has long been known that nuclear size scales with cell size (Wilson, 1925). The scaling relationship is not always perfectly proportional (i.e., isometric) but often reveals a subproportional relationship known as an allometric relationship (Needleman, 2009; Chan and Marshall, 2010).

The shape of the mitotic spindle is a good model for studying scaling inside the cell. The mitotic spindle is a supramolecular apparatus crucial for accurate chromosome segregation during cell division. At metaphase, the microtubules emanating from the centrosomes (poles) capture the chromosomes and align these to the equator between two centrosomes; finally, the diamond-shaped structure of the spindle is constructed. Previous studies suggested a tight link between spindle length and spindle width. The spindle length is the distance between two centrosomes, and the spindle width is the width of the microtubules, perpendicular to the spindle axis, at the center of the spindle where the metaphase plate is positioned. Mechanical manipulation of in vitro–reconstructed metaphase spindles, using *Xenopus* egg extract or in vivo mitotic spindles in mammalian Ptk2 cells, demonstrated that the aspect ratio of the spindle, which is the ratio of the width to the length, remained constant after the manipulation or

This article was published online ahead of print in MBoC in Press (http://www.molbiolcell.org/cgi/doi/10.1091/mbc.E12-07-0528) on March 6, 2013.

*Present address: Genome Biology Unit, European Molecular Biology Laboratory, Heidelberg 69117, Germany.

Address correspondence to: Akatsuki Kimura (akkimura@nig.ac.jp).

Abbreviations used: GFP, green fluorescent protein; HL, hypotenuse length; HSL, half–spindle length; RNAi, RNA interference; SW, spindle width.

© 2013 Hara and Kimura. This article is distributed by The American Society for Cell Biology under license from the author(s). Two months after publication it is available to the public under an Attribution–Noncommercial–Share Alike 3.0 Unported Creative Commons License (http://creativecommons.org/licenses/by-nc-sa/3.0).

"ASCB®," "The American Society for Cell Biology®," and "Molecular Biology of the Cell®" are registered trademarks of The American Society of Cell Biology.

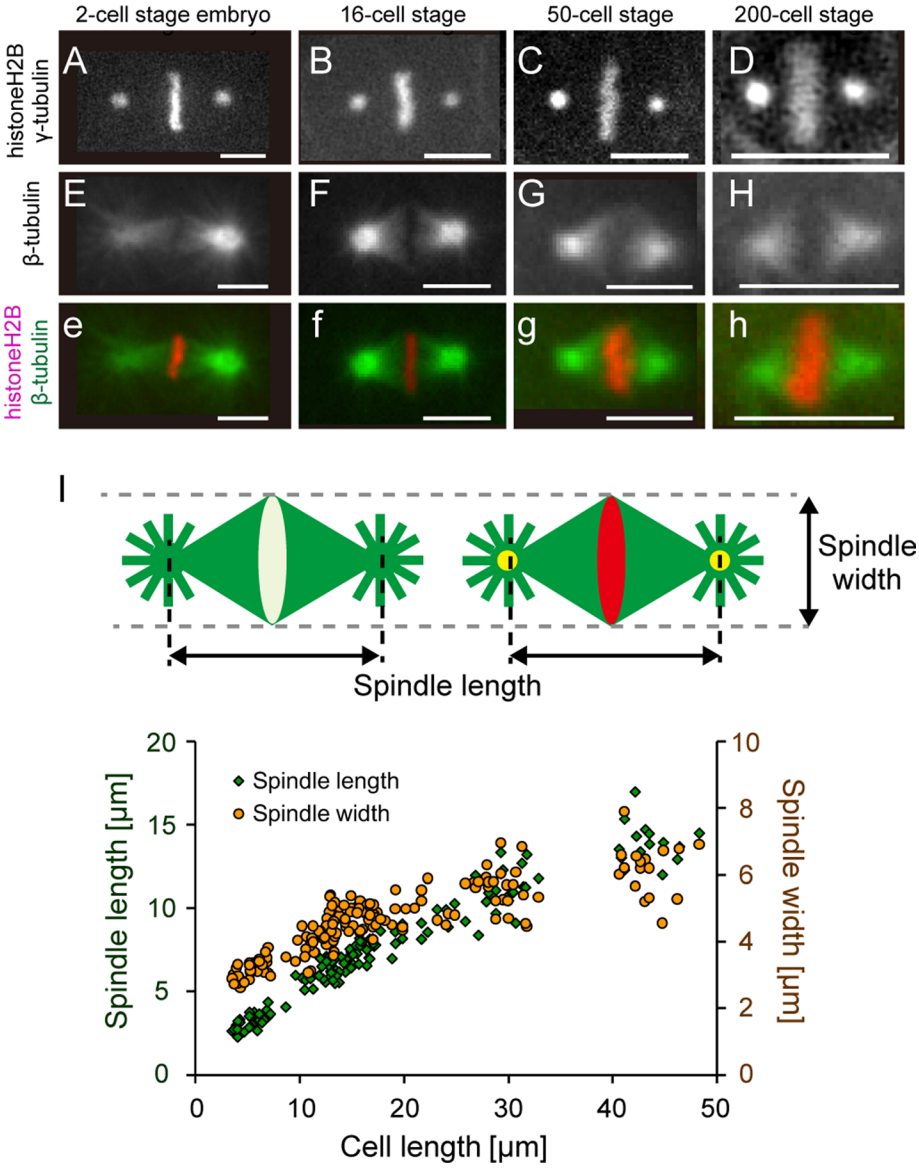

FIGURE 1: Spindle shape during embryogenesis in *C. elegans*. (A–H, e–h) Microscopic images of metaphase spindles at four representative cell stages. (A–D) Chromosomes and centrosomes were simultaneously visualized by GFP–histone H2B and GFP–γ-tubulin. (E–H, e–h) Microtubules and chromosomes of spindles with similar sizes as in A–D were visualized by GFP-tubulin and mCherry–histone H2B. Only microtubules (E–H) or both microtubules (green; e–h) and chromosomes (red; e–h) are shown. (A, E, e) The 2-, (B, F, f) 16-, (C, G, g) 50-, and (D, H, h) 200-cell stage embryos. Bar, 5 μm. (I) The length (green diamonds) and width (yellow circles) of the metaphase spindles plotted against the cell length in wild-type embryos. Schematics show the structure of the *C. elegans* mitotic spindle and illustrate the definitions of spindle width and length used in this study. Microtubules, chromosomes, and the centrosome are shown with green, red, and yellow, respectively. Spindle length was defined as the distance between the centers of two centrosomes visualized by GFP–γ-tubulin. Spindle width is the width of microtubules at the equatorial plane and is identical to the long axis of the GFP-histone–positive region (metaphase plate) in the *C. elegans* embryo.

compression of the spindle (Dumont and Mitchison, 2009; Itabashi *et al.*, 2009). When spatial conformation of the metaphase plate was predetermined by deposited arrays of DNA-coated beads, the length of the reconstructed spindle depended on the spindle width to take on a constant aspect ratio (Dinarina *et al.*, 2009). These observations suggested that the spindle self-organizes to maintain a constant aspect ratio between the spindle length and spindle width.

The dimensions of the metaphase spindle, in particular, the spindle length, are known to vary greatly within species during development (Wühr *et al.*, 2008; Hara and Kimura, 2009; Greenan *et al.*, 2010), as well as among species (Goshima and Scholey, 2010). However, little is known about the relationship between spindle length and spindle width under natural conditions. Does the aspect ratio remain constant among different-sized spindles within a species? Are there any rules regulating the spindle length and spindle width, such that one can be predicted from the other? What kind of mechanical model accounts for the relationship between spindle length and spindle width?

To address these issues, we focused on the mitotic spindles that appear during the embryogenesis of *Caenorhabditis elegans*. During this embryogenesis, the spindle length is altered and correlates with cell size (Hara and Kimura, 2009; Greenan *et al.*, 2010). In this study, we quantified the length and width of the mitotic spindle with various sizes and conditions in an effort to deduce an equation that can empirically calculate spindle width as a function of spindle length in *C. elegans* embryos.

RESULTS

Systematic quantification of spindle width from the 1- to 200-cell stage during embryogenesis in *C. elegans*

To characterize the shape of the metaphase spindle in *C. elegans* embryos, we first observed the spindle at metaphase in various blastomeres. To observe the spindle, we visualized DNA and centrosomes by green fluorescent protein (GFP)–histone H2B and GFP–γ-tubulin, respectively (Figure 1, A–D). In this study, spindle length was defined as the distance between the centers of two centrosomes visualized by GFP–γ-tubulin and spindle width as the width of the microtubules at the center of the spindle, where the metaphase plate was positioned. In *C. elegans*, spindle width is identical to the diameter of the metaphase plate (the long-axis length of the GFP-histone–positive region), owing to the holocentric chromosomes (Figure 1, E–I). We therefore took the diameter of the metaphase plate as the spindle width. As embryogenesis proceeded, cell size and spindle length became shorter, as reported previously (Figure 1I; Hara and Kimura, 2009). As expected, the spindle width also became shorter as embryogenesis proceeded (Figure 1I). In contrast, the change in the thickness of the metaphase plate (length perpendicular to the spindle width) was small compared with the apparent change in the spindle width (Supplemental Figure S1).

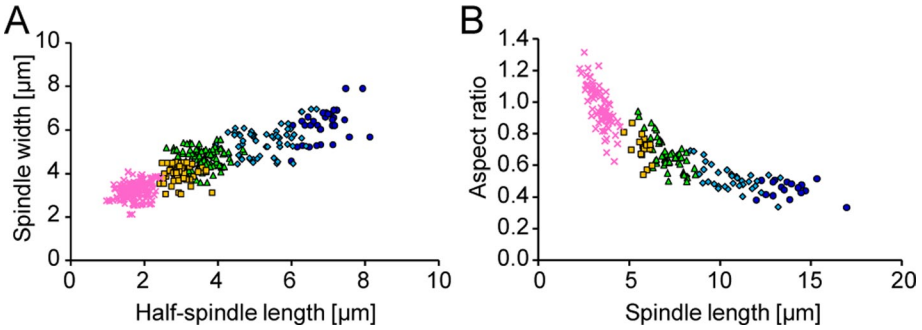

FIGURE 2: Relationship between spindle width and spindle length in *C. elegans*. (A) Relationship between spindle width and half–spindle length in *C. elegans* embryos. (B) The calculated aspect ratio of spindle width/length plotted against the spindle length in *C. elegans* embryos. Color shows the data at different cell stages. Blue circles, 1-cell stage; light blue diamonds, 2- and 4-cell stages; green triangles, 8- and 16-cell stages; yellow rectangles, 28-cell stage; and pink crosses, 50-cell and later stages.

Aspect ratio of spindle length to spindle width is not constant

To analyze the relationship between spindle width and length, we compared the spindle width with the half–spindle length, which is the distance between the chromatin and the centrosome (Figure 2A). As expected, the spindle width correlated well with the spindle length. Next we investigated whether the aspect ratio of the metaphase spindle (calculated by dividing the spindle width by the spindle length) is constant (Figure 2B). Although the calculated aspect ratio was relatively constant for large spindles, the ratio increased as the spindle length decreased; the aspect ratio in later embryonic stages was approximately twofold larger than that in earlier stages (ratio in the 1-cell stage, 0.45 ± 0.05; in the 100-cell stage, 1.02 ± 0.15; Supplemental Table S1). This change in the aspect ratio suggested that the spindle shape changes during embryogenesis. This change is also apparent in the images of the shapes in metaphase spindle (Figure 1).

Spindle width depends on spindle length

Next we investigated whether spindle width depends on spindle length. To this end, we made shorter spindles by using RNA interference (RNAi) to partially deplete TPXL-1 or SPD-2. In *C. elegans* early embryos, it was reported that the amount of TPXL-1 in the centrosome controls spindle length (Ozlu *et al.*, 2005; Greenan *et al.*, 2010). Although severe depletion of TPXL-1 causes deformation of the metaphase spindle, partial RNAi knockdown of *tpxl-1* results in reduced spindle length (Greenan *et al.*, 2010). Similarly, partial RNAi knockdown of *spd-2* results in the reduction of TPXL-1 on the centrosome by reducing the size of the centrosome (Greenan *et al.*, 2010). We quantified both the spindle width and the half–spindle length in each RNAi embryo at the one-cell stage (Figure 3, A–C, and Supplemental Table S2). We found that the spindle width was significantly shorter in RNAi embryos than in wild-type embryos at the one-cell stage (*tpxl-1* [RNAi], 5.0 ± 0.7 μm, $p < 0.001$; *spd-2* [RNAi], 5.2 ± 0.3 μm, $p < 0.005$; Figure 3B). Of importance, the width of the spindle was reduced in these RNAi embryos, to a level comparable to that of the wild-type embryo spindle at later cell stages (Figure 3C). The change in spindle width in these RNAi embryos did not accompany a change in cell length, nuclear size, or individual chromosome size (Figure 3, D–F), supporting the notion that spindle length directly affects spindle width. In addition, it appears unlikely that the developmental stage is a direct determinant of spindle width, because the width of later-stage spindles was reproduced by shortening the spindle length at the one-cell stage (Figure 3C). These results indicated that the spindle length is a direct determinant of spindle width.

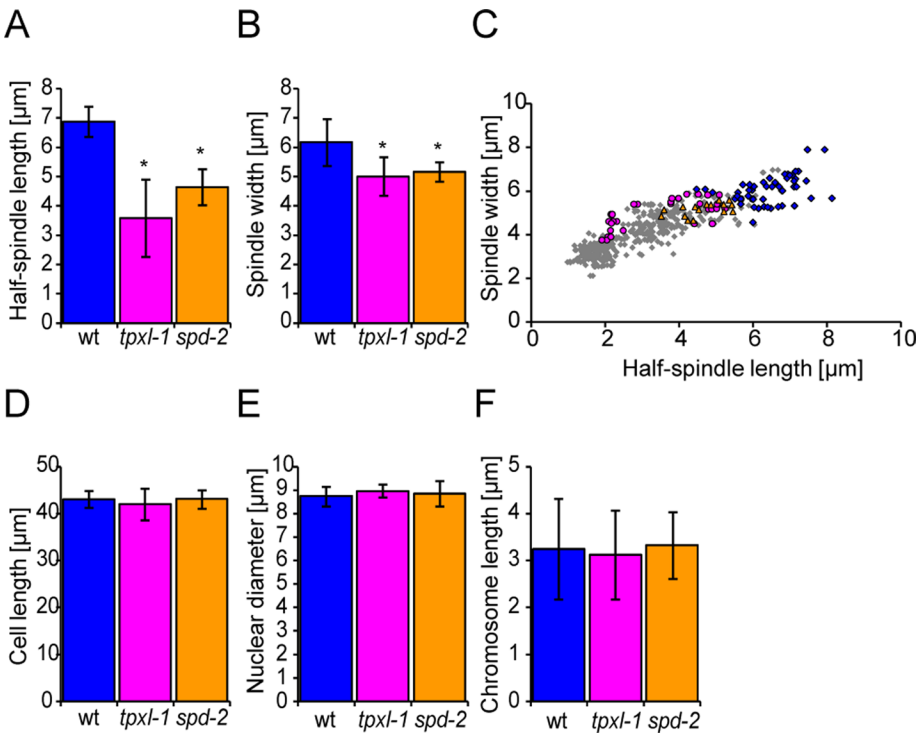

FIGURE 3: Manipulation of spindle length. Half–spindle length (A), spindle width (B), cell length (D), nuclear diameter (E), and chromosome length (F) of one-cell-stage wild-type (wt, blue), *tpxl-1* (RNAi) (pink), and *spd-2* (RNAi) (yellow) embryos are shown. Error bar, SD. The half–spindle length and spindle width for both in *tpxl-1* (RNAi) and *spd-2* (RNAi) embryos are significantly different from those of wild-type embryos (*$p < 0.005$). These mean values are listed in Supplemental Table S2. (C) Relationship between spindle width and half–spindle length in *tpxl-1* (RNAi) and *spd-2* (RNAi) embryos. Data from *tpxl-1* (RNAi) embryos (pink circles) or *spd-2* (RNAi) embryos (yellow triangles) at the one-cell stage are plotted against data of wild-type (gray diamonds) embryos. Blue diamond shows data from only wild-type embryos at the one-cell stage.

Changing spindle width by manipulating quantity of DNA

We then examined how spindle length responded to the change in spindle width, by

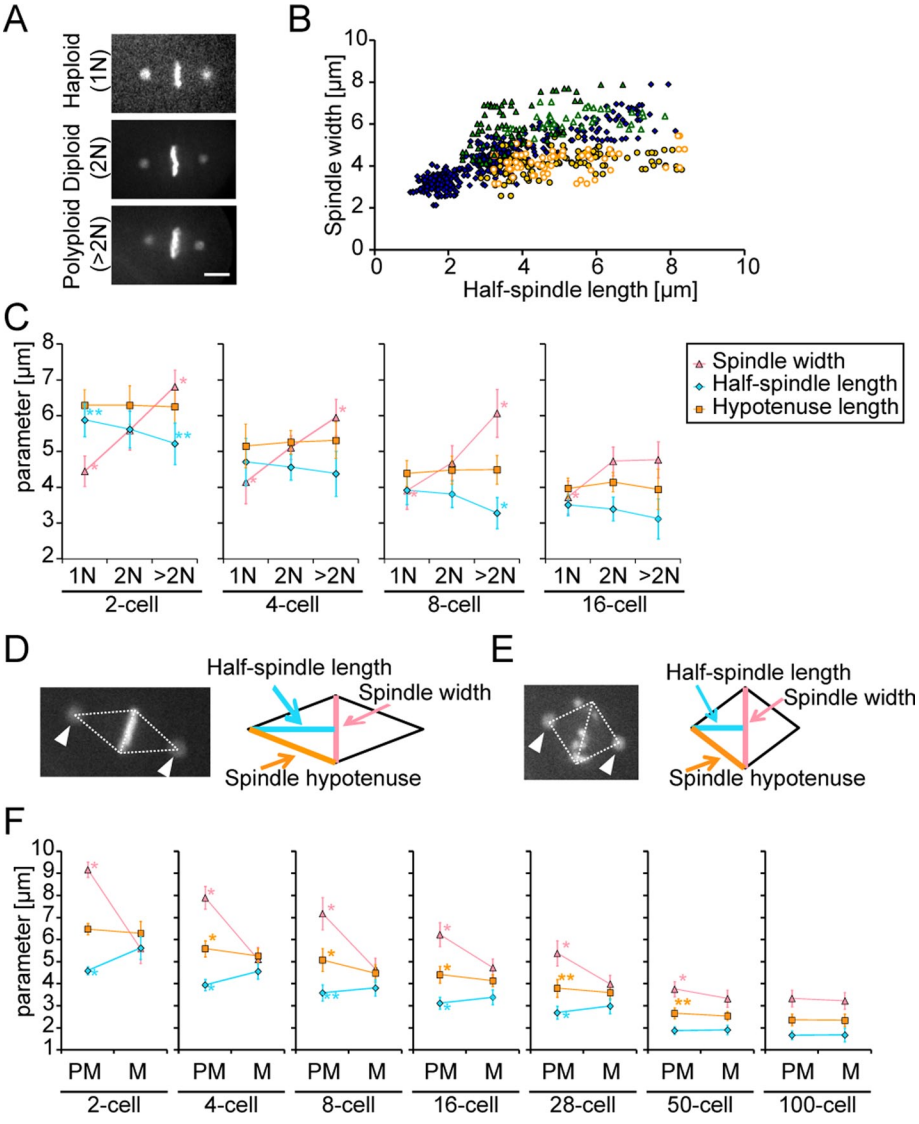

FIGURE 4: Manipulation of DNA quantity and calculation of the hypotenuse length of the spindle. (A) Microscopic images of embryos with different ploidy at the two-cell stage. The control embryos are those with a diploid genome. RNAi for *klp-18*, *ani-1*, or *mei-1* occasionally induced haploid and polyploid (DNA in excess of the diploid genome) embryos. The images are of two-cell-stage embryos at metaphase treated with RNAi for *klp-18*. Bar, 5 μm. (B) Relationship between spindle width and length in embryos with different ploidy. The data of each embryo are shown using different symbols. Blue diamonds, wild-type diploid; yellow circles, *klp-18* (RNAi) haploid; yellow open circles, *mei-1* (RNAi) haploid; green triangles, *klp-18* (RNAi) polyploid; and green open triangles, *ani-1* (RNAi) polyploid. (C) The spindle width (pink), half–spindle length (light blue), and hypotenuse length (orange) at the 2-, 4-, 8-, and 16-cell stages are shown. Symbols and error bars represent the mean values and SD of each parameter, respectively. The data of haploid (1*N*) and polyploid (>2*N*) embryos include the results of *klp-18* (RNAi), *ani-1* (RNAi), and *mei-1* (RNAi). Statistical differences between the data from haploid or polyploid embryos and those from diploid embryos at each cell stage are shown by asterisks (*$p < 0.005$; **$p < 0.05$). The plotted values are listed in Supplemental Table S3. (D) Microscopic images and schematic figure of the metaphase spindle. The bipolar spindle was assumed to be described by two cones, each attaching at the base plane. The half–spindle length, spindle width, and hypotenuse length of the spindle correspond to the height (light blue), base (pink), and hypotenuse (orange) of each triangle. (E) Microscopic images and schematic figures of prometaphase. The premature spindle was also assumed to be described by two cones, each attaching at the base plane. Spindle parameters were defined as in D. (F) The mean values of spindle width, half–spindle length, and hypotenuse length from the 2- to 100-cell stages are shown. The statistical difference between data from prometaphase (PM) and metaphase (M) at each cell stage is shown by asterisks (*$p < 0.005$; **$p < 0.05$).

manipulating the quantity of DNA. Because the chromosomes occupy the metaphase plate, a reduction in the number of chromosomes should directly decrease the spindle width. To change the amount of DNA in the *C. elegans* embryos, we manipulated the ploidy in the embryos (Figure 4, A–C, and Supplemental Table S3). RNAi depletion of *klp-18*, *mei-1*, or *ani-1* is known to cause failure in meiotic division in the oocyte. As a result, some RNAi embryos extrude the entire maternal complement of DNA as a polar body, whereas other RNAi embryos retain the majority or the entire maternal complement of DNA in the embryo (Mains *et al.*, 1990; Quintin *et al.*, 2003; Segbert *et al.*, 2003; Maddox *et al.*, 2005; Dorn *et al.*, 2010). Thus these RNAi embryos spontaneously had only half the normal amount of DNA (haploid), derived only from the paternal DNA, or had an excess of DNA (polyploid). The different ploidy did not result in any apparent differences in cell size, and the mitotic events appeared normal for several cell divisions after fertilization (Mains *et al.*, 1990; Quintin *et al.*, 2003; Segbert *et al.*, 2003; Maddox *et al.*, 2005; Dorn *et al.*, 2010).

Spindle width and length were also correlated with each other in the haploid and polyploid embryos (Figure 4B). In the haploid embryos, the spindle width was shorter than that in the control diploid embryos with the same spindle length. In contrast, the spindle width in the polyploid embryos was longer than that in diploid embryos with the same spindle length. Note that the haploid embryos generated by knocking down either *klp-18* or *mei-1* induced a similar quantitative change in spindle width (Figure 4B). Therefore the effect of knockdown of these molecules on spindle size is likely mediated through the change in DNA quantity rather than by other effects specific to each gene. In addition, RNAi of *klp-18* stochastically produced haploid, diploid, or polyploid cells (Segbert *et al.*, 2003). When we measured the spindle width for each of these embryos, we observed shorter width for haploid cells and longer width for polyploid cells. We concluded that changes in the quantity of DNA in the cell induced changes in spindle width.

Decreasing spindle width in haploid cells results in increasing spindle length

We also quantified the changes in spindle length in haploid and polyploid spindles at each developmental stage. The width of the spindle in haploid embryos was

smaller than that in control diploid embryos, but the spindle length was longer (Figure 4C). On the other hand, in polyploid embryos, the spindle width was longer, whereas the length was shorter, than that of the control embryos (Figure 4C). We assumed that ploidy directly affects spindle width but not spindle length, because here spindle width equals the radius of the metaphase chromatin plate. These results suggest that changes in spindle length induced by changing ploidy were mediated through changes in spindle width, that is, spindle width could induce changes in spindle length.

Length of the spindle hypotenuse remains constant at each cell stage

Because the decreases in spindle width were accompanied by increases in spindle length when manipulating the ploidy, we hypothesized that the length of the "hypotenuse" in the spindle might remain constant. The shape of the metaphase spindle can be approximated as two circular cones, each attached to the base plane (Figure 4D). We coined the term "hypotenuse length" to describe the length of the line connecting the centrosome and the edge of the metaphase plate. The hypotenuse length (*HL*) was calculated from the half–spindle length (*HSL*) and the spindle width (*SW*) using a simple Pythagorean theorem, $HL^2 = HSL^2 + (SW/2)^2$ (Figure 4D). First, we compared the hypotenuse length among embryos with different ploidy at each developmental stage. The calculated hypotenuse lengths were not significantly different among spindles with different quantities of DNA (Figure 4C; orange), whereas both the spindle length and spindle width were different (Figure 4C; light blue and pink).

In addition to the metaphase spindle, we calculated the hypotenuse length during the course of spindle formation (Figure 4E and Supplemental Table S4). From prometaphase to metaphase, the spindle length increased and the spindle width decreased at each developmental stage (Figure 4F; light blue and pink). In contrast, the hypotenuse lengths remained almost constant during spindle formation, although the hypotenuse length was different for each developmental stage (Figure 4F; orange).

These findings indicate that whereas hypotenuse length is stable during spindle formation regardless of ploidy, it is dependent on embryonic stage. The regulatory mechanism underlying hypotenuse length is unknown; however, centrosome size may set hypotenuse length. Centrosome size, which depends on the amount of centrosomal proteins such as TPXL-1 and SPD-2, correlates with spindle length and is believed to regulate the spindle length directly (Greenan *et al.*, 2010). Centrosome size decreases as the cell divides due to conservation of total material (Decker *et al.*, 2011), which can explain the reduction in spindle length during embryogenesis (Goehring and Hyman, 2012). Because spindle length is largely proportional to hypotenuse length, particularly until the 16-cell stage (Supplemental Figure S2A), where centrosome size–dependent regulation of spindle length has been proposed (Greenan *et al.*, 2010), a centrosome size–dependent mechanism may also explain the hypotenuse length. Of interest, centrosome size at metaphase was constant when we manipulated ploidy, suggesting a closer correlation with hypotenuse length than with spindle length at metaphase (Supplemental Figure S2B). Furthermore, both centrosome size and hypotenuse length are constant from prometaphase to metaphase after the four-cell stage (Decker *et al.*, 2011; Figure 4F and Supplemental Figure S2C). Thus far, the only exception to this is the transition from prometaphase to metaphase at the two-cell stage, where centrosome size increases (Decker *et al.*, 2011; Supplemental Figure S2C). Therefore hypotenuse length correlates very well, but not perfectly, with centrosome size. However, we cannot refute the possibility that conservation of hypotenuse length occurs due to the conservation of other cellular parameters. Note that, unlike in yeast (Ding *et al.*, 1993), mass is not conserved in spindles with different lengths (Supplemental Figure S2, D and E). The conservation of hypotenuse length might be a consequence of combinatorial changes in spindle length and width upon ploidy changes, mediated by changes in microtubule dynamics and its association with chromosomes.

Allometric relationship between spindle width, hypotenuse length, and ploidy

We showed that spindle width depends on spindle length and ploidy. Although spindle length depended on the amount of DNA, the hypotenuse length did not. Therefore the spindle width should be a function of two independent parameters, namely, the hypotenuse length and the DNA quantity. First, to clarify the relationship between hypotenuse length and spindle width, we plotted hypotenuse length against spindle width (Figure 5A). In the double-logarithmic plot, the hypotenuse length correlated well with spindle width in diploid embryos. The slope of the regression line for the diploid plot was 0.58. Because the slope of the double-logarithmic plot did not approximate 1, the relationship between the spindle width and the hypotenuse length is not isometric but is instead allometric (Chan and Marshall, 2010). We confirmed this relationship by plotting the spindle width as a function of the 0.58 power of the hypotenuse length (Figure 5B). In this graph, the data fitted the regression line, given as $SW = 2.0 \times HL^{0.58}$. On the other hand, the regression line for haploid embryo data, including the data from *mei-1* (RNAi) and *klp-18* (RNAi) haploid embryos, is described by $SW = 1.5 \times HL^{0.58}$ (Figure 5B).

Thus data from diploid and haploid cells fitted well to $SW = \alpha \times HL^{0.58}$, where the proportionality constant α is different for diploid ($\alpha_{diploid} = 2.0$) and haploid ($\alpha_{haploid} = 1.5$) cells. We further assumed a power-law scaling relationship between α and ploidy and obtained $\alpha \propto P^{0.36}$, where P is the ploidy number (Figure 5C). The relationship between spindle width and ploidy was also allometric. According to this assumption, data from both diploid and haploid cells should fit the equation $SW = \beta \times P^{0.36} \times HL^{0.58}$. To calculate the constant β, we replotted *SW* for both haploid and diploid spindles against $P^{0.36} \times HL^{0.58}$ (Figure 5D). Regression analysis indicated that $SW = 1.5 \times P^{0.36} \times HL^{0.58}$ best fitted the data both from haploid and diploid embryos (Figure 5D).

To test the predictive performance of this equation, we estimated the ploidy from *SW* and *HL* of the polyploid spindles that we had measured in *klp-18* (RNAi) or *ani-1* (RNAi) embryos (Figure 4, A–C). The ploidy number for each spindle was estimated from $P = [SW/(1.5 \times HL^{0.58})]^{2.8}$. The average ploidy number for all polyploid spindles is estimated as 3.3 ± 1.1, which is significantly larger than 2 (diploid). In addition, we estimated the individual ploidy number of *klp-18* (RNAi) polyploid embryos and *ani-1* (RNAi) embryos as $P_{klp\text{-}18\ (RNAi)} = 3.7 \pm 1.1$ and $P_{ani\text{-}1(RNAi)} = 2.7 \pm 0.6$, respectively. This estimation supports the notion that the average amount of DNA in *klp-18* (RNAi) polyploid embryos is higher than that in *ani-1* (RNAi) embryos. Indeed, all *ani-1* (RNAi) embryos that possessed additional maternal DNA frequently extruded variable amounts of maternal DNA as polar bodies (Maddox *et al.*, 2005), whereas some *klp-18* (RNAi) polyploid embryos never produced any polar bodies. When we plotted the spindle widths in polyploid embryos against $P^{0.36} \times HL^{0.58}$, using the estimated ploidy number in each *klp-18* (RNAi) and *ani-1* (RNAi) embryo, the

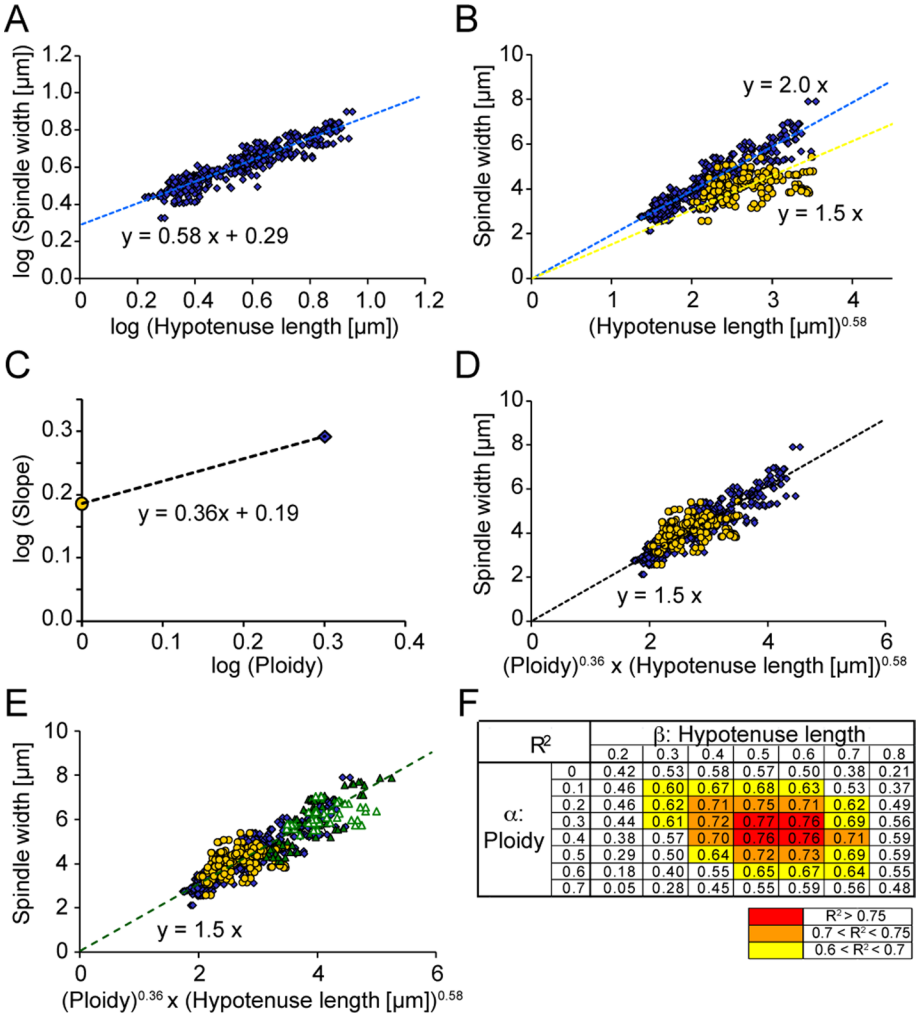

FIGURE 5: An allometric relationship between spindle width, hypotenuse length and ploidy. (A) Double-logarithmic plot between spindle width and hypotenuse length in wild-type diploid embryos. (B) The spindle width is plotted against the 0.58 power of hypotenuse length in diploid (blue diamonds) and haploid (yellow circles) embryos. Regression lines for the data of each diploid and haploid embryo are shown. (C) The slopes of each regression line shown in C are plotted against ploidy in a double-logarithmic graph. (D) The spindle width is plotted against $P^{0.36} \times HL^{0.58}$. A regression line is shown for all data from diploid (blue diamond) and haploid (yellow circle) embryos. (E) The value of ploidy in polyploid embryos was calculated using the relationship described in D. With this value, the spindle width was recalculated and plotted (green triangles) as in D. A regression line is shown for data only from polyploid embryos. (F) R^2 calculated using plots of SW against $P^{\alpha} \times HL^{\beta}$ and listed for variations in the exponents of α and β. The background colors represented the strength of R^2.

data fitted the same line as for the haploid and diploid cells (Figure 5E). Therefore this simple equation appears to describe variation in spindles; from this equation, spindle width can be estimated from the hypotenuse length and the ploidy.

Possible range of power-law exponents in the equation

We obtained the equation $SW = 1.5 \times P^{0.36} \times HL^{0.58}$, which best fits our present measurements. To investigate the possible range of the power-law exponents in the equation that significantly fitted the data, we plotted SW against $P^{\alpha} \times HL^{\beta}$ with various combinations of α and β near the best-fit value. For each plot, we performed regression analysis and calculated the coefficient of determination (R^2) for each combination of α and β (Figure 5F). Although the exponents with best fit ($\alpha = 0.36$ and $\beta = 0.58$) had $R^2 = 0.77$, it held that $R^2 > 0.6$ for a range of $\alpha = 0.1$–0.6 and $\beta = 0.3$–0.7.

DISCUSSION

This is the first systematic characterization of the relationship between the spindle width, length, and hypotenuse in mitotic spindles of various sizes using *C. elegans* embryos. Our analysis shows that the width and hypotenuse of spindles in the *C. elegans* embryo are described by $SW = 1.5 \times P^{0.36} \times HL^{0.58}$, where SW is spindle width, P is ploidy, and HL is hypotenuse length. We can estimate spindle width once we know ploidy and hypotenuse length, which depend on cell stage, TPXL-1, and SPD-2. Once hypotenuse length and spindle width are determined, we can calculate spindle length (SL) using a Pythagorean theorem, $(SW/2)^2 + (SL/2)^2 = HL^2$. The formula means that spindle width shows a sublinear dependence on spindle hypotenuse, as $SW \propto HL^{0.58}$. This sublinear dependence, or allometry, is often described as a power-law relationship $y \propto x^{\alpha}$, where α is smaller or greater than 1 (Chan and Marshall, 2010). An allometric relationship is often observed in scaling between two cellular parameters (Wühr *et al.*, 2008; Hara and Kimura, 2009) and thus may be a general feature of the construction of cellular architecture.

We observed that hypotenuse length is maintained constant during each cell stage (Figure 4). How is hypotenuse length linked to mechanical control of spindle width? On the basis of the observation that chromosomes are tightly packed into a relatively small metaphase plate within the spindle from prometaphase to metaphase, we assumed that spindle microtubules must have a "squeezing effect" on spindle width. Spindle microtubules are known to be cross-linked to each other (Compton, 1998; Burbank *et al.*, 2007). Such an attractive force between spindle microtubules would account for the proposed squeezing force. Because spindle width is shorter when the hypotenuse length is shorter (Figure 5A), the squeezing force should correlate negatively with the hypotenuse length. Such a hypotenuse length–dependent squeezing force might be related to the antibending force of the elastic microtubules, as longer elastic rods would have less resistance to bending.

We also demonstrated that DNA ploidy affects spindle width. Because the increase in chromosome number induces widening of the spindle, we assume mutual repulsion of chromosomes. One apparent source of the repulsive force is steric hindrance: because a chromosome occupies a certain volume at the metaphase plate, an increase in chromosome number would result in steric hindrance at the metaphase plate. In addition, metaphase chromosomes behave as elastic material (Marshall *et al.*, 2001; Bouck and Bloom, 2007; Marko, 2008) and thus may generate repulsive forces.

From the obtained equation, a possible force-balance model for regulation of spindle width can be derived. We hypothesize that at the kinetochores along the direction of the metaphase plate, a

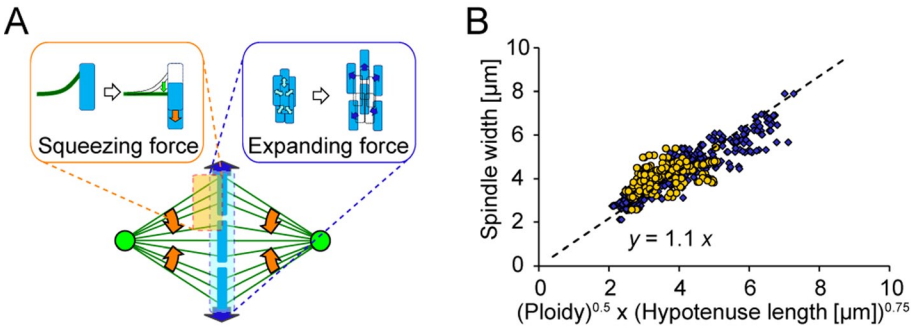

FIGURE 6: Force-balance model to set the spindle width. (A) Schematic of our proposed model. The force balance between a squeezing force (orange arrow) and expanding force (blue arrow) determines the spindle width. In generating the squeezing force (left inset), the microtubule attached to the chromosome is assumed to act as would an elastic rod. When the microtubule is bent by moving the chromosomes to the outside (i.e., increasing the chromosome number), the microtubule tends to straighten. Because the other end of the microtubule is tethered tightly at the centrosome, the force generated by straightening of the microtubule induces the chromosome to move to the inside the spindle, thus compressing the spindle width. For generating an expanding force (right inset), interchromosome repulsion is assumed. When chromosomes are tightly packed (i.e., with increasing chromosome numbers), the chromosomes tend to move away from each other due to this repulsive force. This movement induces an expansion of the metaphase plate. (B) The calculated $P^{0.5} \times HL^{0.75}$ values, based on our proposed model, plotted against spindle width for diploid (blue diamonds) and haploid (yellow circles) embryos. The regression line and its equation are described on the graph. $R^2 = 0.64$.

balance between squeezing by kinetochore microtubules and expansion of the metaphase plate determines spindle width (Figure 6A). For the squeezing force, which depends on the length of the spindle hypotenuse, we modeled a kinetochore microtubule as a bending elastic rod. When an elastic rod is bent in one direction, the rod generates a force in the opposite direction (Figure 6A). The force F is expressed as $F = 3EI \times y/L^3$, where L is the length of the rod, y is the deflection, and EI is the flexural rigidity (Howard, 2001). Although the equation is valid only when the deflection is small and the other end of the rod is clamped, we approximated that the kinetochore microtubule–dependent force squeezing the metaphase plate would be proportional to spindle width and inversely proportional to the cubic length of the kinetochore microtubule (i.e., the hypotenuse length); that is, $F \propto SW/HL^3$ per microtubule. Considering that the force would act on the entire metaphase plate, and assuming the plate to be circular with a perimeter of πSW, the total force squeezing the metaphase plate can be modeled as $F \propto SW^2/HL^3$. In this model, kinetochore microtubules are assumed to bend inward, which is the direction opposite to the bend known to be adopted by microtubules in fusiform spindles. The fusiform shape has been explained as being caused by the outward bend of the interpolar microtubules when they are pushed by each other in a direction perpendicular to the metaphase plate (Rubinstein *et al.*, 2009). We assume that kinetochore microtubules are bent inward and interpolar microtubules are bent outward; in total, the spindle appears fusiform.

With regard to the force driving expansion of the metaphase plate, we assumed that the chromosomes repulse each other (Figure 6A). To model the repulsion force between two chromosomes, we assumed that the force would be inversely proportional to the square of the distance, in analogy to the repulsion between electrically charged particles (Phillips *et al.*, 2009). Theoretically, the force required to confine N repulsive particles to a cylindrical plate of radius R and thickness L can be formulated as $F \propto N^2/LR^2$ (Phillips *et al.*, 2009). Because N, the number of repulsive particles (i.e., chromosomes), should be proportional to ploidy, P, the force to expand the metaphase plate can be modeled as $F \propto \sim P^2/SW^2$.

The force balance between squeezing and expansion is therefore described as $SW^2/HL^3 \propto P^2/SW^2$, and thus $SW \propto P^{0.5} \times HL^{0.75}$. This relationship is similar to the one we obtained from the experimental quantification ($SW \propto P^{0.36} \times HL^{0.58}$), and the exponents are within the range of a high determination coefficient ($R^2 = 0.64$; Figure 6B). This force-balance regulation can therefore explain the scaling feature of spindles that we observed in this study. This is the only model we have to explain the equation, but we recognize that other models might be possible.

Several features we observed in the *C. elegans* embryo may not apply to other species. In yeast, a change in ploidy does not induce a change in spindle length (Storchova *et al.*, 2006). Previous observations in mice and *Xenopus* do not support a negative correlation between the aspect ratio of the spindle and the spindle length (Supplemental Table S5). In mice, the mass of the microtubule-organizing centers decreases throughout embryogenesis, whereas spindle length remains rather constant (Courtois *et al.*, 2012). This diversity might be a reflection of diversity in the organization of metaphase spindles among organisms (Goshima and Scholey, 2010).

We demonstrated that the amount of DNA present in the cell significantly affects spindle shape (Figure 4C). This finding implies that differences in genome size should have a significant effect on spindle shape in different species. However, when we plotted spindle width against the calculated hypotenuse length for various species and cell types, we found good correlation between the spindle width and the hypotenuse length, regardless of the marked variability in genome size (Supplemental Figure S3, A–C). Why should spindles from various species with differing amounts of DNA have a similar shape (Supplemental Figure S3D)? We speculate that spindle shape should be similar, regardless of the species, for efficient chromosome segregation. To compensate for the diversity in genome sizes, different species adopt different mechanism for spindle formation (Goshima and Scholey, 2010). Further studies should investigate how these differences contribute mechanically to spindle shape to resolve why spindle shape is similar among species.

MATERIALS AND METHODS

C. elegans strains and RNAi procedure

To observe the metaphase spindle and the cell membrane, we use the CAL0061 strain, which expresses GFP–γ-tubulin (*tbg-1*), GFP–histone H2B (*his-11*), and GFP–PHPLCdelta-1 (Hara and Kimura, 2009). To visualize the individual chromosomes, we used the N2 strain. For RNAi, double-strand RNAs were prepared and injected as described previously (Kimura and Onami, 2005; Kimura and Kimura, 2011). For partial RNAi depletion, we set the incubation times from the injection of the dsRNA to observation to 3–5 h (for *tpxl-1* [RNAi]) or 5–6 h (for *spd-2* [RNAi]), based on the results of a time course for RNAi depletion (Pecreaux *et al.*, 2006; Greenan *et al.*, 2010). Primer sequences for *tpxl-1, klp-18*, and *ani-1* RNAi were used as described in previous studies (Segbert *et al.*, 2003; Maddox *et al.*, 2005; Ozlu *et al.*, 2005), and those for *spd-2* and *mei-1* RNAi were obtained from the PhenoBank database (worm .mpi-cbg.de/phenobank2; Sonnichsen *et al.*, 2005).

Imaging and measurement

To observe individual cells inside the embryo, as well as the metaphase spindle, we simultaneously visualized the centrosome, chromosomes, and cell membrane in embryos of the CAL0061 strain as previously described (Hara and Kimura, 2009). The size parameters (cell length, spindle length, and spindle width) at metaphase were quantified as follows. First, we selected the image at metaphase from the time-lapse image sequence (30-s intervals) as the image obtained just before the onset of chromosome segregation in anaphase. Cell length and spindle length were defined as the length of the longest axis of the cell and the distance between the centers of two centrosomes, respectively, as previously reported (Hara and Kimura, 2009). A half–spindle length was defined as the distance between the center of centrosome and that of the chromatin. Spindle width was measured as the length along the GFP-histone–positive metaphase plate. The diameter of the nucleus at prophase was quantified as follows. We selected the image at prophase as the image obtained immediately before breakdown of the nuclear envelope, which was detected by diffusion of free GFP-histone signals from the nucleus to cytoplasm. The accurate length and width of the prometaphase spindle were difficult to quantify directly because the two centrosomes (spindle poles) move dynamically and chromosomes do not align at this stage. We therefore defined the length and width of the prometaphase spindle as the diameter of the prophase nucleus. The parameters were measured using the line scan tool on ImageJ (National Institutes of Health, Bethesda, MD). For visualization of microtubules within the spindle, we used a tubulin::GFP; histone::mCherry strain (CAL0491; Hayashi *et al.*, 2012). Individual chromosomes were observed by slight modifications of standard procedures (Albertson and Thomson, 1982; Yoshida *et al.*, 1984). The detailed procedure of the observation will be published elsewhere (Y.H. *et al.*, unpublished data).

Statistical analysis

We performed simple regression analysis using Excel software (Microsoft, Redmond, WA) to draw regression lines. Evaluation for correlation was obtained from calculation of R^2. We used the two-sided Student's *t* test to determine the significance of differences between two groups, as previously described (Hara and Kimura, 2009).

ACKNOWLEDGMENTS

We thank Jon Audhya (University of Wisconsin, Madison, WI) for providing some strains; Kazuo Yamagata (Osaka University, Osaka, Japan) for providing unpublished mouse imaging data sets; and Takeshi Itabashi (Waseda University, Tokyo, Japan), François Nédélec (European Molecular Biology Laboratory, Heidelberg, Germany), and members of the Cell Architecture Laboratory for helpful discussions. Some nematode strains used in this work were provided by the *Caenorhabditis* Genetics Center, which is funded by the National Institutes of Health National Center for Research Resources. Y.H. is a Research Fellow of the Japan Society for the Promotion of Science. This study was supported by grants from the Ministry of Education, Culture, Sports, Science, and Technology, Japan.

REFERENCES

Albertson DG, Thomson JN (1982). The kinetochores of *Caenorhabditis elegans*. Chromosoma 86, 409–428.

Bouck DC, Bloom K (2007). Pericentric chromatin is an elastic component of the mitotic spindle. Curr Biol 17, 741–748.

Burbank KS, Mitchison TJ, Fisher DS (2007). Slide-and-cluster models for spindle assembly. Curr Biol 17, 1373–1383.

Chan YH, Marshall WF (2010). Scaling properties of cell and organelle size. Organogenesis 6, 88–96.

Compton DA (1998). Focusing on spindle poles. J Cell Sci 111, 1477–1481.

Courtois A, Schuh M, Ellenberg J, Hiiragi T (2012). The transition from meiotic to mitotic spindle assembly is gradual during early mammalian development. J Cell Biol 198, 357–370.

Decker M, Jaensch S, Pozniakovsky A, Zinke A, O'Connell KF, Zachariae W, Myers E, Hyman AA (2011). Limiting amounts of centrosome material set centrosome size in *C. elegans* embryos. Curr Biol 21, 1259–1267.

Dinarina A, Pugieux C, Corral MM, Loose M, Spatz J, Karsenti E, Nédélec F (2009). Chromatin shapes the mitotic spindle. Cell 138, 502–513.

Ding R, McDonald KL, McIntosh JR (1993). Three-dimensional reconstruction and analysis of mitotic spindles from the yeast, *Schizosaccharomyces pombe*. J Cell Biol 120, 141–151.

Dorn JF, Zhang L, Paradis V, Edoh-Bedi D, Jusu S, Maddox PS, Maddox AS (2010). Actomyosin tube formation in polar body cytokinesis requires anillin in *C. elegans*. Curr Biol 20, 2046–2051.

Dumont S, Mitchison TJ (2009). Compression regulates mitotic spindle length by a mechanochemical switch at the poles. Curr Biol 19, 1086–1095.

Goehring NW, Hyman AA (2012). Organelle growth control through limiting pools of cytoplasmic components. Curr Biol 22, R330–R339.

Goshima G, Scholey JM (2010). Control of mitotic spindle length. Annu Rev Cell Dev Biol 26, 21–57.

Greenan G, Brangwynne CP, Jaensch S, Gharakhani J, Julicher F, Hyman AA (2010). Centrosome size sets mitotic spindle length in *Caenorhabditis elegans* embryos. Curr Biol 20, 353–358.

Hara Y, Kimura A (2009). Cell-size-dependent spindle elongation in the *Caenorhabditis elegans* early embryo. Curr Biol 19, 1549–1554.

Hara Y, Kimura A (2011). Cell-size-dependent control of organelle sizes during development. Results Probl Cell Differ 53, 93–108.

Hayashi H, Kimura K, Kimura A (2012). Localized accumulation of tubulin during semi-open mitosis in the *Caenorhabditis elegans* embryo. Mol Biol Cell 23, 1688–1699.

Howard J (2001). Mechanics of Motor Proteins and the Cytoskeleton, Sunderland, MA: Sinauer.

Itabashi T, Takagi J, Shimamoto Y, Onoe H, Kuwana K, Shimoyama I, Gaetz J, Kapoor TM, Ishiwata S (2009). Probing the mechanical architecture of the vertebrate meiotic spindle. Nat Methods 6, 167–172.

Kalab P, Heald R (2008). The RanGTP gradient—a GPS for the mitotic spindle. J Cell Sci 121, 1577–1586.

Katsura I (1990). Mechanism of length determination in bacteriophage lambda tails. Adv Biophys 26, 1–18.

Kimura A, Onami S (2005). Computer simulations and image processing reveal length-dependent pulling force as the primary mechanism for *C. elegans* male pronuclear migration. Dev Cell 8, 765–775.

Kimura K, Kimura A (2011). Intracellular organelles mediate cytoplasmic pulling force for centrosome centration in the *Caenorhabditis elegans* early embryo. Proc Natl Acad Sci USA 108, 137–142.

Levy DL, Heald R (2010). Nuclear size is regulated by importin alpha and Ntf2 in *Xenopus*. Cell 143, 288–298.

Maddox AS, Habermann B, Desai A, Oegema K (2005). Distinct roles for two *C. elegans* anillins in the gonad and early embryo. Development 132, 2837–2848.

Mains PE, Kemphues KJ, Sprunger SA, Sulston IA, Wood WB (1990). Mutations affecting the meiotic and mitotic divisions of the early *Caenorhabditis elegans* embryo. Genetics 126, 593–605.

Marko JF (2008). Micromechanical studies of mitotic chromosomes. Chromosome Res 16, 469–497.

Marshall WF (2004). Cellular length control systems. Annu Rev Cell Dev Biol 20, 677–693.

Marshall WF, Marko JF, Agard DA, Sedat JW (2001). Chromosome elasticity and mitotic polar ejection force measured in living *Drosophila* embryos by four-dimensional microscopy-based motion analysis. Curr Biol 11, 569–578.

Moseley JB, Mayeux A, Paoletti A, Nurse P (2009). A spatial gradient coordinates cell size and mitotic entry in fission yeast. Nature 459, 857–860.

Needleman DJ (2009). Cellular allometry: the spindle in development and inheritance. Curr Biol 19, R846–847.

Ozlu N, Srayko M, Kinoshita K, Habermann B, O'Toole ET, Muller-Reichert T, Schmalz N, Desai A, Hyman AA (2005). An essential function of the *C. elegans* ortholog of TPX2 is to localize activated aurora A kinase to mitotic spindles. Dev Cell 9, 237–248.

Pecreaux J, Roper JC, Kruse K, Jülicher F, Hyman AA, Grill SW, Howard J (2006). Spindle oscillations during asymmetric cell division require a threshold number of active cortical force generators. Curr Biol 16, 2111–2122.

Phillips R, Kondev J, Theriot J (2009). Physical Biology of the Cell, New York: Garland.
Quintin S, Mains PE, Zinke A, Hyman AA (2003). The mbk-2 kinase is required for inactivation of MEI-1/katanin in the one-cell *Caenorhabditis elegans* embryo. EMBO Rep 4, 1175–1181.
Rubinstein B, Larripa K, Sommi P, Mogilner A (2009). The elasticity of motor-microtubule bundles and shape of the mitotic spindle. Phys Biol 6, 016005.
Segbert C, Barkus R, Powers J, Strome S, Saxton WM, Bossinger O (2003). KLP-18, a Klp2 kinesin, is required for assembly of acentrosomal meiotic spindles in *Caenorhabditis elegans*. Mol Biol Cell 14, 4458–4469.
Sonnichsen B *et al*. (2005). Full-genome RNAi profiling of early embryogenesis in *Caenorhabditis elegans*. Nature 434, 462–469.
Storchova Z, Breneman A, Cande J, Dunn J, Burbank K, O'Toole E, Pellman D (2006). Genome-wide genetic analysis of polyploidy in yeast. Nature 443, 541–547.
Varga V, Leduc C, Bormuth V, Diez S, Howard J (2009). Kinesin-8 motors act cooperatively to mediate length-dependent microtubule depolymerization. Cell 138, 1174–1183.
Wilson EB (1925). The Cell in Development and Heredity. New York: Macmillan.
Wühr M, Chen Y, Dumont S, Groen AC, Needleman DJ, Salic A, Mitchison TJ (2008). Evidence for an upper limit to mitotic spindle length. Curr Biol 18, 1256–1261.
Yoshida TH, Sadaie T, Sadaie Y (1984). Somatic and meiotic chromosomes of the small free-living nematode, *Caenorhabditis elegans*. Proc Japan Acad 60, 54–57.